Journal of Al-Azhar University Engineering Sector

Vol. 18, No. 69, October 2023, 786- 804

Nonlinear Analysis of the Gusset Plate Connection for Braced Frames Subjected to Monotonic and Cyclic Loading

Mohamed B. Abel Wahab[1,*], Mohamed A. Galal[1], Emad S. Salem[1,2]

[1]Civil Engineering Department, Faculty of Engineering, Al-Azhar University, Cairo, Egypt

[2]Construction Engineering, Faculty of Engineering, Galala University, Suze, Egypt

*Correspondence: ceng.muhammedbahaa1990@gmail.com

Citation:

M. B. Abel Wahab, M. A. Galal, and E. S. Salem, "Nonlinear Analysis of the Gusset Plate Connection for Braced Frames Subjected to Monotonic and Cyclic Loading", Journal of Al Azhar University Engineering Sector, vol. 18, pp. 786-804, 2023.

Received: 09 Sep. 2023

Accepted: 12 Oct. 2023

DoI: 10.21608/auej.2023.235226.1422

ABSTRACT

In this paper, studies on braced frames are presented to study their behavior under the influence of seismic loads. Steel braced frame systems are considered an efficient and economical technique to resist horizontal and to maintain the lateral deformation of buildings under the effect of wind and seismic loads. Among these studies, a study was conducted at the University of California - Berkeley, America, in 2012-2013 by Lai and Mahin. This study conducted laboratory tests for three full-scale one-bay two-story braced frames with different cross sections for the braces such as square-HSS, circular-HSS and wide-flange I beam. A three-dimensional model is conducted to validate the laboratory test, using ABAQUS program. In this model, non-linear material properties are used for each part of the model. Two types of loading are developed, nonlinear static and nonlinear dynamic. A comparison is made between the results of the experimental test and the numerical model, which showed that good agreement between these results.

KEYWORDS : Experimental test, Finite element modeling, Monotonic loading, Cyclic loading, braced frames, gusset plate connections.

التحليل اللاخطي لوصلات الألواح المجمعة للإطارات ذات الشكالات المعرضة للتحميل الأحادي والدوري

محمد بهاء الدين عبد الوهاب[1،*]، محمد أحمد جلال[1]، عماد سعيد سالم[1،2]

[1] قسم الهندسة المدنية - كلية الهندسة ، جامعة الازهر، القاهرة ، مصر

[2] هندسة التشييد - كلية الهندسة ، جامعة الجلالة، السويس، مصر

*البريد الاليكتروني للباحث: E-mail ceng.muhammedbahaa1990@gmail.com

الملخص العربي:-

في هذا البحث، تم تقديم الدراسات التي أجريت علي الأطارات الفراغية ذات الشكالات لدراسة سلوكها تحت تأثير أحمال الزلازل. ومن هذه الدراسات، دراسة أجريت في جامعة كالفورنيا – بيركلي بأميريكا عام 2012 – 2013 بواسطة كلا من لاي وماهين. وقد قامت هذه الدراسة بإختبارات معملية لثلاث نماذج كاملة بقطاعات مختلفة للشكالات التي بداخل هذه الإطارات. وقد تم عمل نموذج ثلاثي الأبعاد لأحد هذه النماذج التي استخدمت في الإختبارات المعملية بواسطة برنامج الأباكس. وقد استخدم في هذا النموذج خصائص المواد الغير خطية لكل جزء من أجزاء النموذج. وقد تم التأثير علي النموذج بنوعين من الأحمال، أحدهما خطي والأخر دوري. وقد تم عمل مقارنة بين نتائج الأختبار العملي والنموذج العددي والتي أظهرت اتفاقا جيدا بين هذه النتائج.

الكلمات المفتاحية : الأختبار المعملي ، نمذجة العناصر المحدودة ، التحميل الأحادي ، التحميل الدوري ، الأطارات ذات الشكالات و وصلات ألواح التقوية.

1. INTRODUCTION

Steel braced frame systems are considered an efficient and economical technique to resist horizontal and to maintain the lateral deformation of buildings under the effect of wind and seismic loads. There are many shapes of braced frames such as single diagonal, chevron, diamond, single-X, stacked-X and split-X as shown in Fig. 1. Braced frames divided into three main types according to configuration [1] : Concentrically braced frames (CBF), Non-concentrically braced frames (NCBF) and Eccentrically braced frames (EBF) as shown in Fig. 2 and Fig. 3. The buckling restrained braced frame (BRBF) is a special type of CBF because the braces do not buckle when loaded in compression. Special concentrically braced frame (SCBF) is a type of (CBF) with additional detailing requirements to provide high energy dissipation capacity and to resist ductility under inelastic deformations. One of these requirements is the connections that should be designed on the force demands that obtained from the maximum expected forces of the brace in tension and compression [1]. There are many researchers conducted their research on the components of the braced frames to improve the behavior of these braced frames under highly seismic zones.

One of the components of the braced frames is the bracing member. The bracing member will buckle under compression loads and yield under tension loads, which make the behavior of these member's complex. There are many research study the performance of multi-story braced frame either numerical or experimental have been conducted on the multi-story braced frames.

The second components of the braced frames is the connections. One of these connections are the connections between the brace member to the beam and the column which called gusset plate connections. Many studied the connections performance in terms of the distribution of forces as well as the buckling of the gusset plate under compression loads and yielding under tension loads.

The American institute of steel construction (AISC) 1984 [3] presented a AISC method to design the gusset plate connection**Error! Reference source not found.**. Richard, R. M. 1986 [4] studies the distribution of forces on the gusset plate. Williams and Richard 1986 [5] studied the importance of frame action effect in the gusset plate-to-frame fastener force distribution. Astaneh-Asl 1989 [6] proposed the Truss analogy method. Thornton, W. A. 1991 [7] verified the experimental results from the task group which formed by AISC and he developed the Uniform force method. Ricker DT 1992 [8] presented the Parallel force method. Thornton WA. 1992 [9] proposed the KISS method (Keep It Simple and Stupid). Astaneh-Asl A. 1998 [10] presented the Concentric force method. Muir LS 2008 [11] proposed the Generalized Uniform Force Method (GUFM) in order to eliminate the constraint that exists in the (UFM). A series of the experimental and analytical investigations has been conducted in University of Washington from 2005 - 2011 to improve and enhance the seismic performance of SCBFs. The research program included single-story, two-story, and three-story tests. Also, more than 30 single-story, single-bay SCBFs were tested to investigate the connection details of the corner gusset plates and present a new balanced design procedure with an elliptical clearance model for the corner gusset plates [12][17]. Ebrahimi et al. 2019 [18] proposed a design procedure for the gusset plate dimensions and force distribution at the interface between the gusset plate to beam and column.

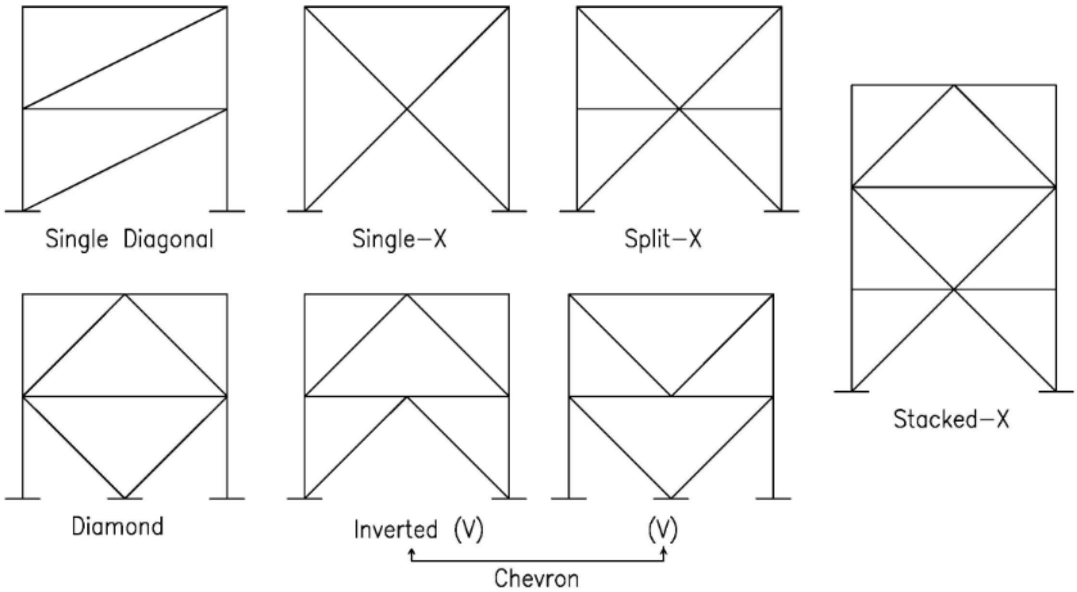

Fig. 1 : Different shapes of braced frames system [1].

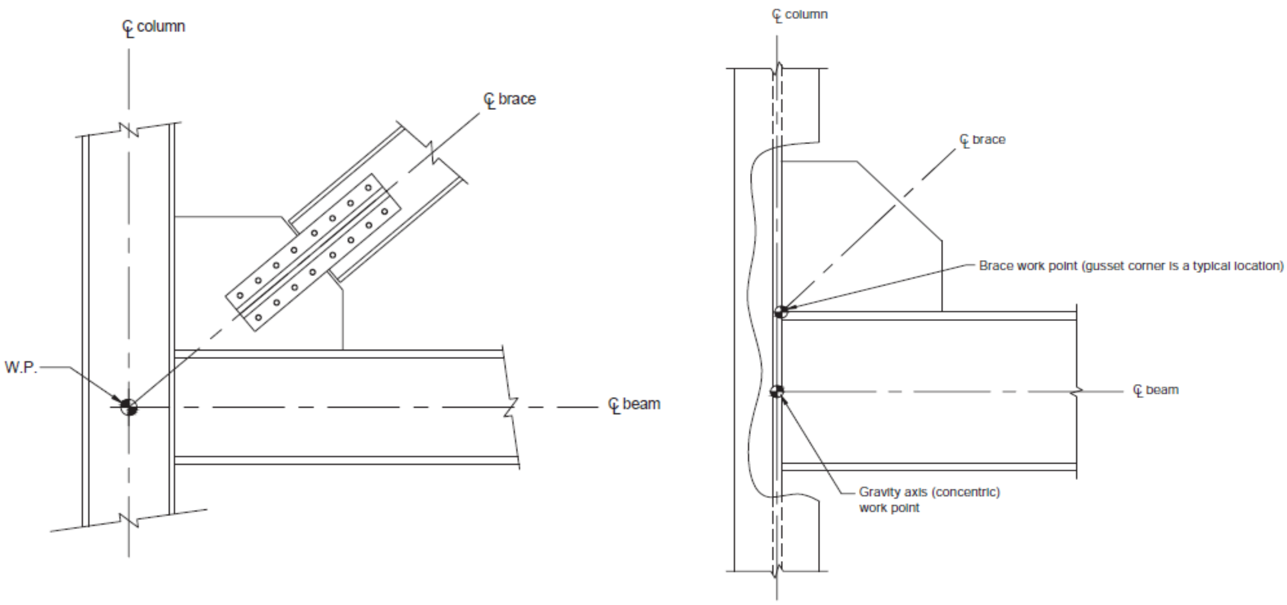

Fig. 2 : Typical concentric gusset connection and nonconcentric brace work point [1].

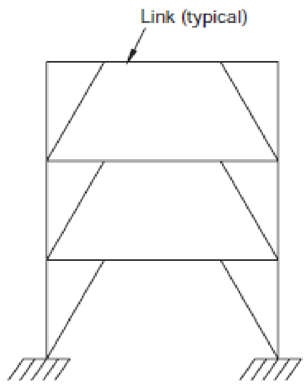

Fig. 3 : Eccentrically braced frame [1].

2. DESCRIPTION OF THE EXPERIMENTAL BRACED FRAME

The test specimen consists of one bay two stories Special concentrically braced frame with the height of stories 9 ft and the span of 20 ft as shown in Fig. 4. Fig. 5 shows the types of members for the test specimen the specimen was tested quasi-statically under cyclic loading. All braces were slotted and welded to the gusset plates as per AISC requirements. Based on these requirements, reinforcing plates were welded to the braces at the net reduced section of the braces at end of the gusset plate.

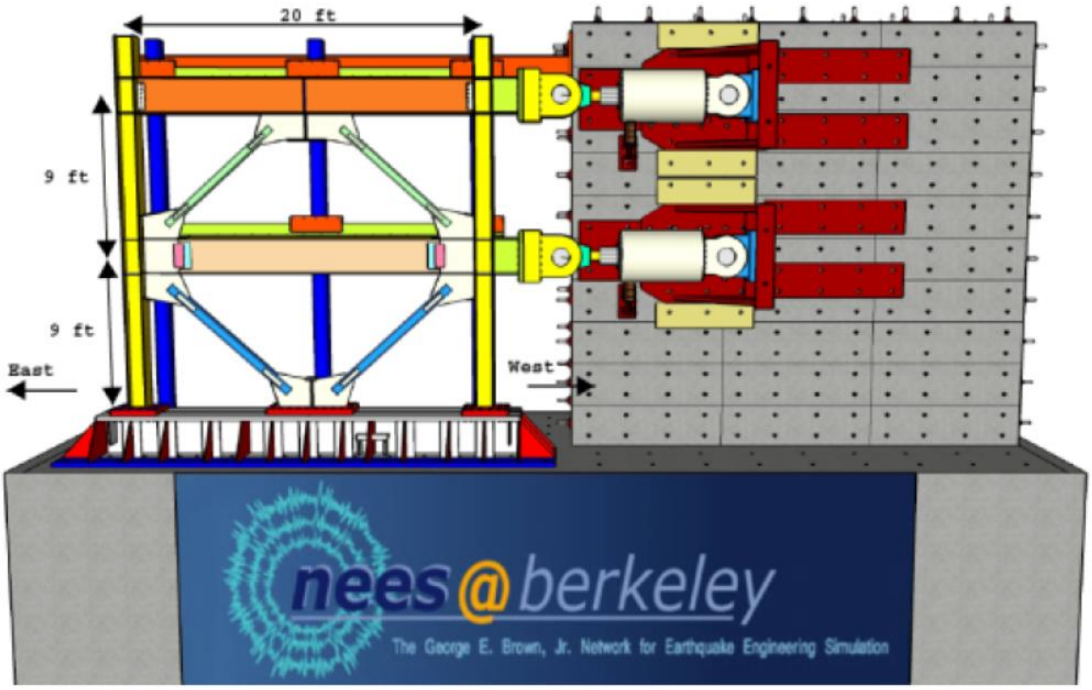

Fig. 4 : Overview and dimension of test specimen TCBF-B-1 [19].

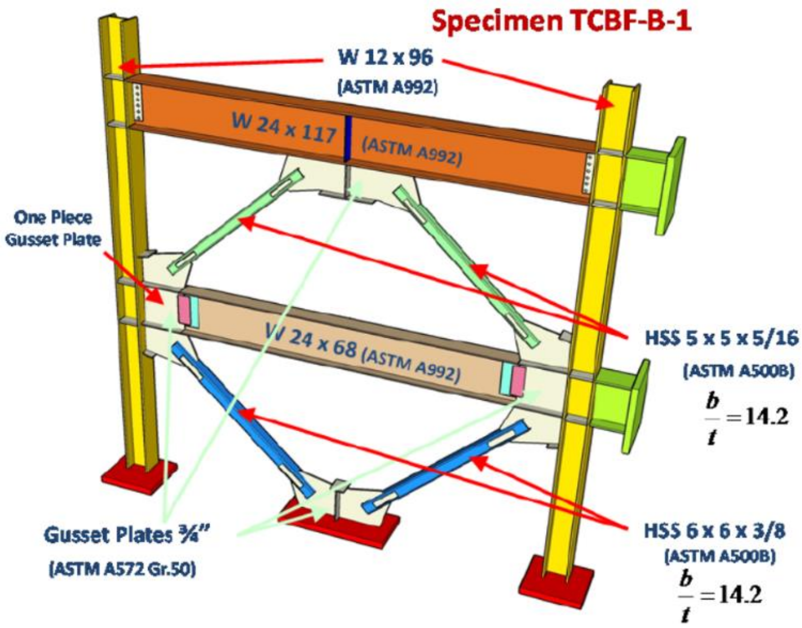

Fig. 5 : Specimen TCBF-B-1 member sizes [19].

Complete joint penetration weld details were specified at the lower beam-to-gusset plate connections. The beam top and bottom flanges were 45° grooved, and welded to gusset plate finger stiffeners. Backing bars were used on the top flange and bottom flange welds and not removed after welding. The beam web was also 45° grooved and welded on one side as shown in Fig. 6**.**

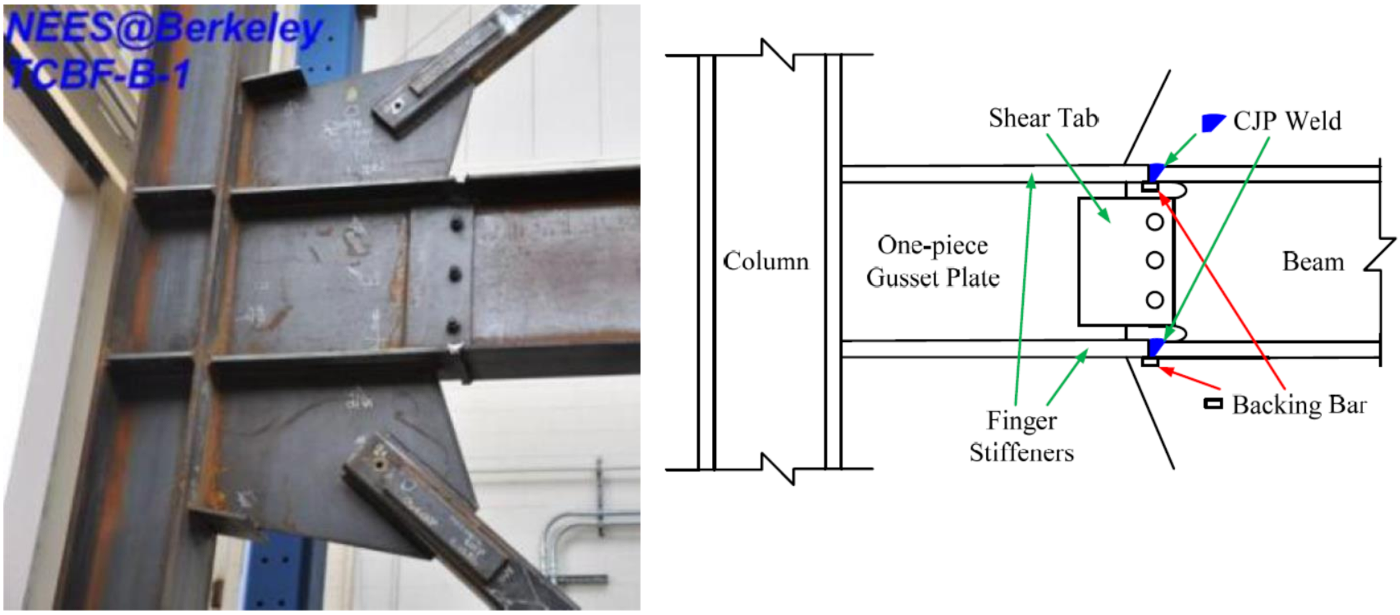

Fig. 7 : Weld details between gusset plate to beam and column [19].

3. FE MODELING

A three-dimensional finite element model for braced frame was developed to simulate the observed experimental test conducted by (Jiun-Wei Lai; Stephen A. Mahin, 2013) [19] using ABAQUS/CAE (version 6.14-4) [20]. Detailed description of the finite elements used, material properties, element type, boundary condition and a comparison between the finite element and experimental results are presented in the following sections.

3.1. MODEL GEOMETRY

Braced Frame Model contains two steel columns, six beams with different lengths, four braces and other parts to tie the columns to the beams. The span between columns 6140 mm (c/c), first story height 2760 mm (c/c) and second story height 2780 mm (c/c) as shown in Fig. 8 and Fig. 9. Basic dimensions and engineering properties of sections used for beams, columns, braces and other parts are listed in Table 1 to Table 3 [1].

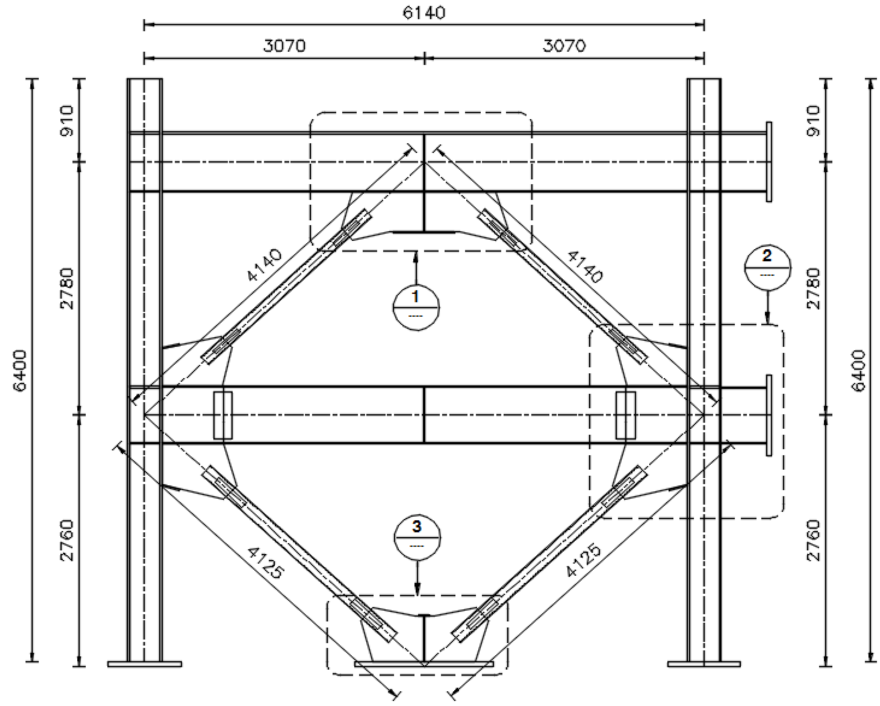

Fig. 8: Model geometry [19].

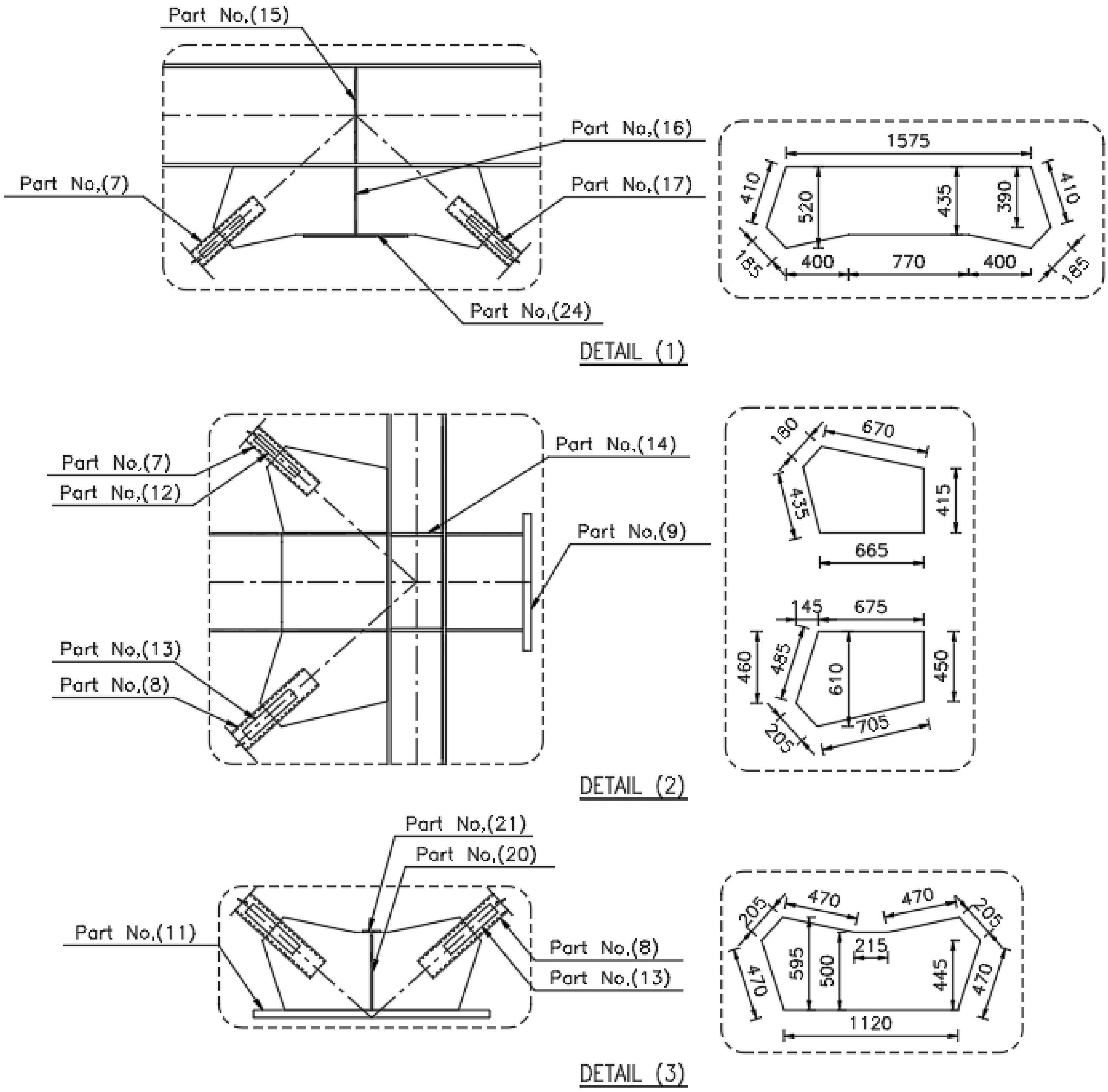

Fig. 9: Details 1, 2 and 3 for the model geometry [19].

Table 1 : Dimensions of columns and beams.

Part No.	Part name	b_f (mm)	t_f (mm)	d_w (mm)	t_w (mm)	Length (mm)
1	Column W(12X96)	330	22	330	14	6400
2	Upper Beam W(24X117)	330	22	616	14	5766
3	Lower Beam W(24X68)	228	14	603.25	11	4406.9
4	Lower Small Beam W(24X68)	228	14	603.25	11	679.55
5	Upper Stub Beam W(24X117)	330	22	616	14	500
6	Lower Stub Beam W(24X68)	228	14	603.25	11	500

Table 2: Dimensions of braces.

Part No,	Part name	Outer width (mm)	Outer depth (mm)	Thickness of box (mm)	Length (mm)
7	Upper brace HSS(5X5X5/16)	120	120	8	2413
8	Lower brace HSS(6X6X3/8)	150	150	9	2751

Table 3: Dimensions of plates and stiffeners.

Part No,	Part name	Width of plate b_p (mm)	Depth of plate d_p (mm)	t_p (mm)
9	Upper and lower stub plate	780	880	50
10	Base plate at column	800	720	50
11	Base plate at middle	1520	650	50
12	(8) Stiffener with upper bracing -(c103)	50	355	16
13	(8) Stiffener with lower bracing-(d103)	75	405	16
14	(16) Stiffener with column-(k100)	165	330	22
15	(2) Stiffener with upper beam-(c102)	165	616	12.5
16	(2) Stiffener with upper gusset plate-(f102)	155.5/107	436.5	12.5
17	Stiffener with upper gusset plate (g102)	230	670	12.5
18	(2) Stiffener with lower beam-(k102)	165	603.25	12.5
19	(4) Stiffener with lower beam-(g100)	203	518	12.5
20	Stiffener with base plate at middle-(h103)	105.5/150.5	500	12.5
21	Stiffener with base plate at middle-(j103)	115	230	12.5
22	All gusset plates	See Details		19

3.2. MATERIAL PROPERTIES

Braced Frame Model contains on four types of steel materials which are ASTM A992, ASTM A572 Grade 50, ASTM A500 Grade B and ASTM A36. All wide flange beams and wide flange columns were made of ASTM A992 steel section. All braces using hollow structural sections (HSS) were made of ASTM A500 Grade B steel tubes for square sections. The gusset plates, base plates, stub beam end plates, shear tabs, finger plates, continuity plates and brace reinforcing cover plates were made of ASTM A572 Grade 50 steel plates. The beam web stiffener plates, lifting lugs, shim plates, and miscellaneous parts were made of ASTM A36 steel plates [19]. The elastic properties of this model are; Young's modulus, E, is 200,000 MPa and Poisson's ratio, υ, is 0.3. When defining materials in ABAQUS [20], the elastic and inelastic material behaviour must be defined. Modulus of elasticity for steel is defined to predict the behaviour of material in the elastic range, while the true stress (σ_{true}) and logarithmic plastic strain (ε^{pl}) are required to define the material after the elastic range.

The following equations are used to convert engineering stress – strain curve to true stress and plastic strain curve in ABAQUS 6.14-4:

$$\sigma_{true} = \sigma_{nom} (1+\varepsilon_{nom}) \qquad 0\text{–}1)$$

$$\varepsilon_{true} = \ln (1+ \varepsilon_{nom}) \qquad 0\text{–}2)$$

$$\varepsilon_{pl} = \varepsilon_{true} - \varepsilon_{el} = \varepsilon_{true} - \sigma_{true} / E \qquad 0\text{–}3)$$

Where:
σ_{true} = true stress, σ_{nom} = engineering (nominal) stress, ε_{nom} = engineering (nominal) strain, ε_{pl} = plastic strain, ε_{true} = true strain, ε_{el} = true elastic strain, E = Young's modulus.

The previous equations were used for all materials defined in the finite element model as shown in Fig. 10.

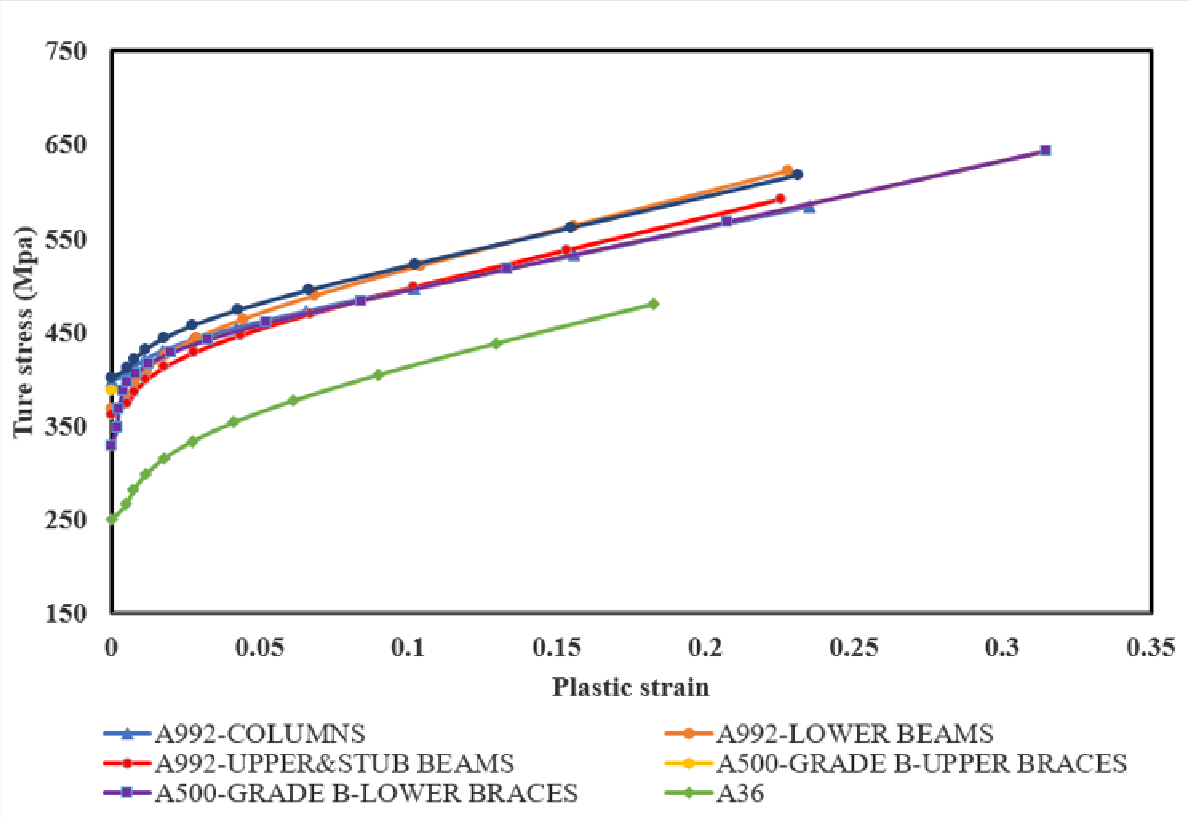

Fig. 10: True stress-strain curves [19].

3.3. ELEMENT TYPE AND MESH SIZE

A four-node shell element, S4R with reduced integration in ABAQUS 6.14-4 [20] was used for all instances to create the finite element model. The S4R element has six degrees of freedom per node, quadrilateral element that is suitable for a wide range of applications and its better convergence rate for the section points through the shell thickness. Before assigning mesh instances, each instance is seeded using seed part technique. For models with complex details, the meshing quality is important. Duplicate mesh elements are needed to get accurate results from a finite element simulation, so it is sometimes necessary to partition the parts to define a better mesh quality. The mesh sizes of the parts are often related to each other. A finer mesh is used in the regions of high stresses or deformation gradients, while a coarser mesh is used in regions of low stresses or deformation gradients. Mesh is refined in gusset plates and bracing members were the stress concentration and deformation are expected as shown in Fig. 11 and Fig. 12.

Fig. 11 : Typical mesh size for ABAQUS model.

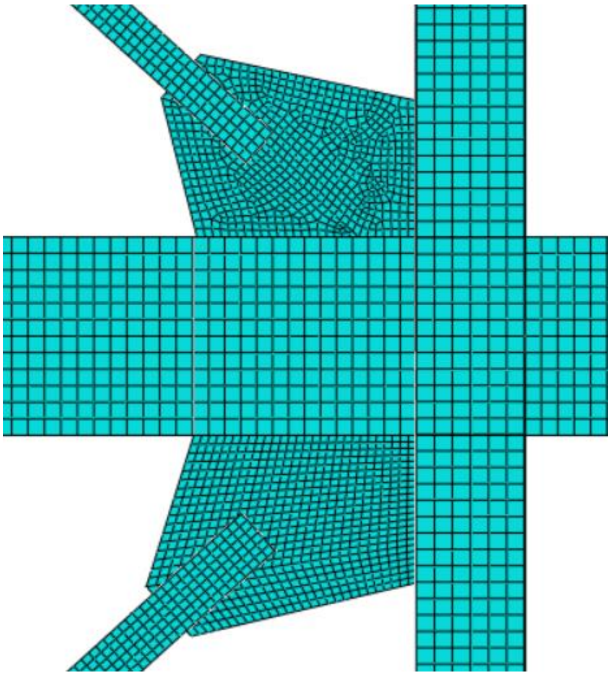

Fig. 12 : Finer mesh for gusset plate connections.

3.4. BOUNDARY CONDITIONS

Boundary conditions in ABAQUS were defined first in the initial step and posted to the next step. The FE model was supported at fifth regions according to the experimental test as shown in Fig. 13. The first and second regions are supported in ABAQUS in six directions (fixed support) and applied at the end of columns. The third region is supported in six directions (fixed support) and applied at the end of lower bracing. The sixth and seventh regions are restraint in z-direction to prevent lateral buckling for the upper and lower beams as shown in Fig. 14.

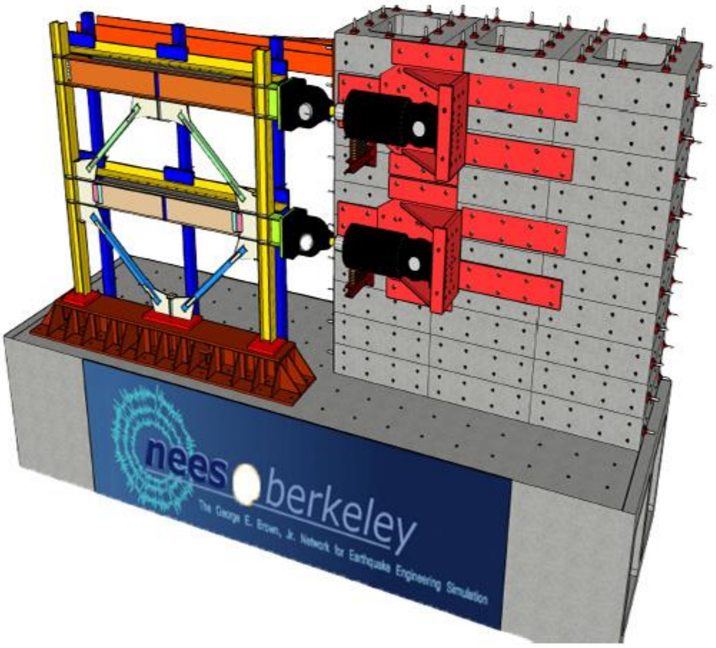

Fig. 13 : Boundary conditions for the experimental test [19].

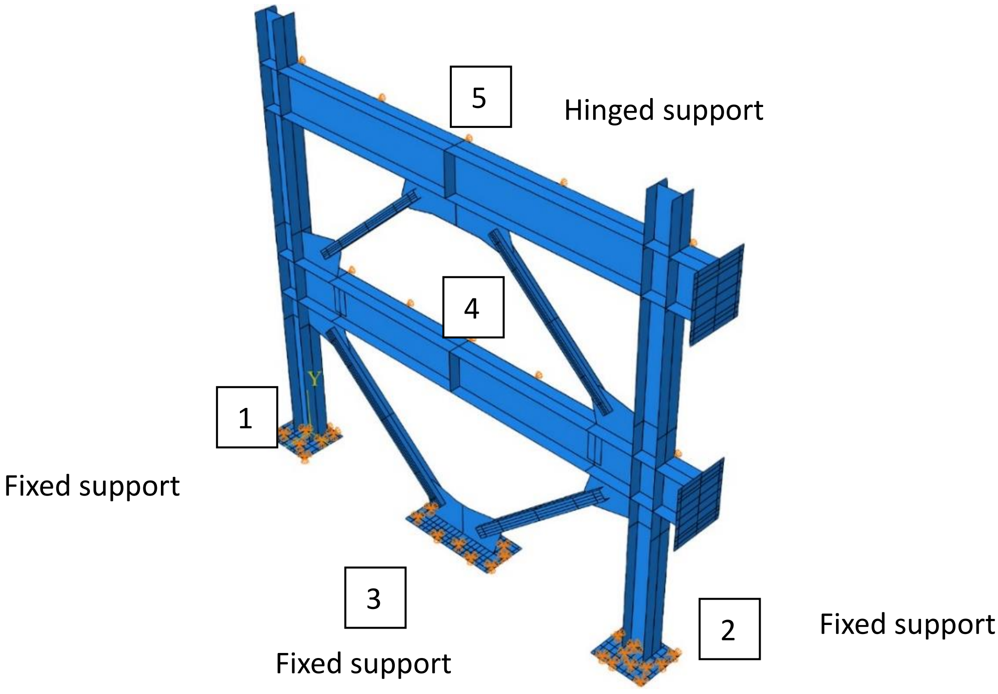

Fig. 14 : Boundary Conditions in ABAQUS Model.

3.5. LOADING APPLICATION AND ANALYSIS METHOD

Loads can define by using the displacement-controlled method or the loading-controlled method. When using of any two methods, the load is incrementally applied to the node or surface. While there is another type of loads which is called the cyclic load. In the cyclic load, the load is applied by a cyclic loading protocol.

Experimental test on the specimen TCBF-B-1 was tested quasi-statically, with a prescribed history of the upper beam displacement imposed. The displacement of the upper beam was monitored and controlled during the entire test process and the lower beam actuator was force controlled. The sign convention for imposed displacements and forces are that positive displacements and forces correspond to the actuator pushing the specimen to the east side of laboratory while negative values correspond to the actuator pulling the specimen to the west side of laboratory [19].

In the FE model, the loads were applied by two methods. The first method was the monotonic loading and the second method was the cyclic loading method.
In the first method, the load applied on the lower beam was one-half of the upper beam. The upper load was 2.6688×10^{6} N (2668.8 kN) while the lower load was 1.3344×10^{6} N (1334.4 kN) as shown in Fig. 15.

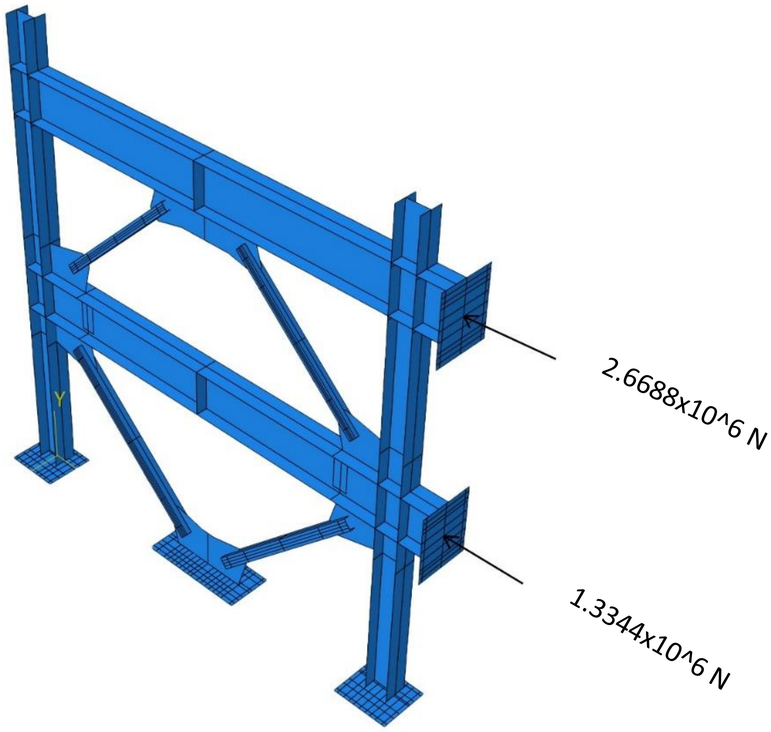

Fig. 15 : Applied loads as a force load in ABAQUS model.

The time step is used to define the analysis steps and take place in two stages. ABAQUS define the initial step by default to apply boundary conditions, but the second step must then define to apply the loadings. In this research one "Static, Riks" procedure was used, in addition to the initial step. When the loads can cause large deformations, the geometric nonlinearity is important, so the 'Nlgeom' option should be turned 'On' to consider the nonlinear geometry effect. The maximum number of increments, initial, minimum and maximum increment size in this research were: 100, 1×10^{-3}, 1×10^{-15}, and 0.5, respectively.

In the second method, the loading protocol has been used to apply the cyclic loading. To apply the loading protocol, the amplitude option in ABAQUS was used to define the cycles of the displacement and time as shown in Fig. 16 [19]. The type of analysis method was considered to be of general static. To apply the load amplitude, two boundary conditions was created. These boundary conditions were of 'Displacement/Rotation' type and restraint it in (x-direction) in the direction of the load. One of these boundary condition was applied at the upper beam while the second boundary condition was applied at the lower beam. In the upper boundary condition, the load amplitude was selected and multiplied by 1 in the (x-direction). In the lower boundary condition, the load amplitude multiplied by 0.5 in the (x-direction) as the lower load was one-half of the upper beam.

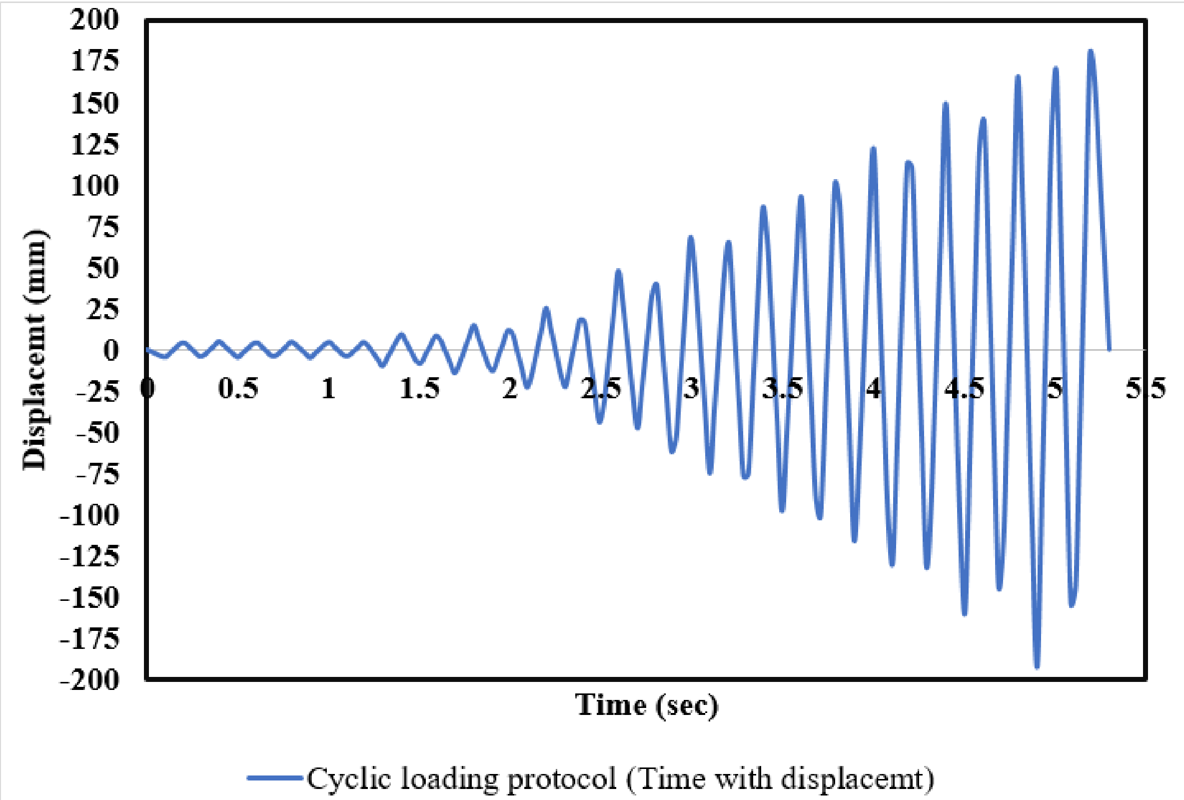

Fig. 16 : Applied cyclic loading protocol in ABAQUS model [19].

3.6. GEOMETRIC IMPERFECTION

Steel Structure members often face some crookedness or other geometric imperfections as a result of the manufacturing, transporting, handling and erection processes. There are two types of geometric imperfections: local and global imperfections. Local imperfections can be found in any region of steel member which cause this region to be yielding stressed, while the global imperfections are along the member length in any direction. The effect of geometric imperfection is taken by applying eigenvalue buckling analysis and the worst case of local and global buckling modes can be determined. To define geometric imperfections in ABAQUS model there are three ways: as a linear superposition of buckling Eigen modes, from the displacements of a static analysis, or by specifying the node number and imperfection. In this research a linear superposition of buckling Eigen modes way was used. The lowest 50 (positive) buckling loads (eigenvalues) and the corresponding buckling shapes (Eigen modes) were determined. Fig. 17 shows the first 4 modes which were taken in the FE model.

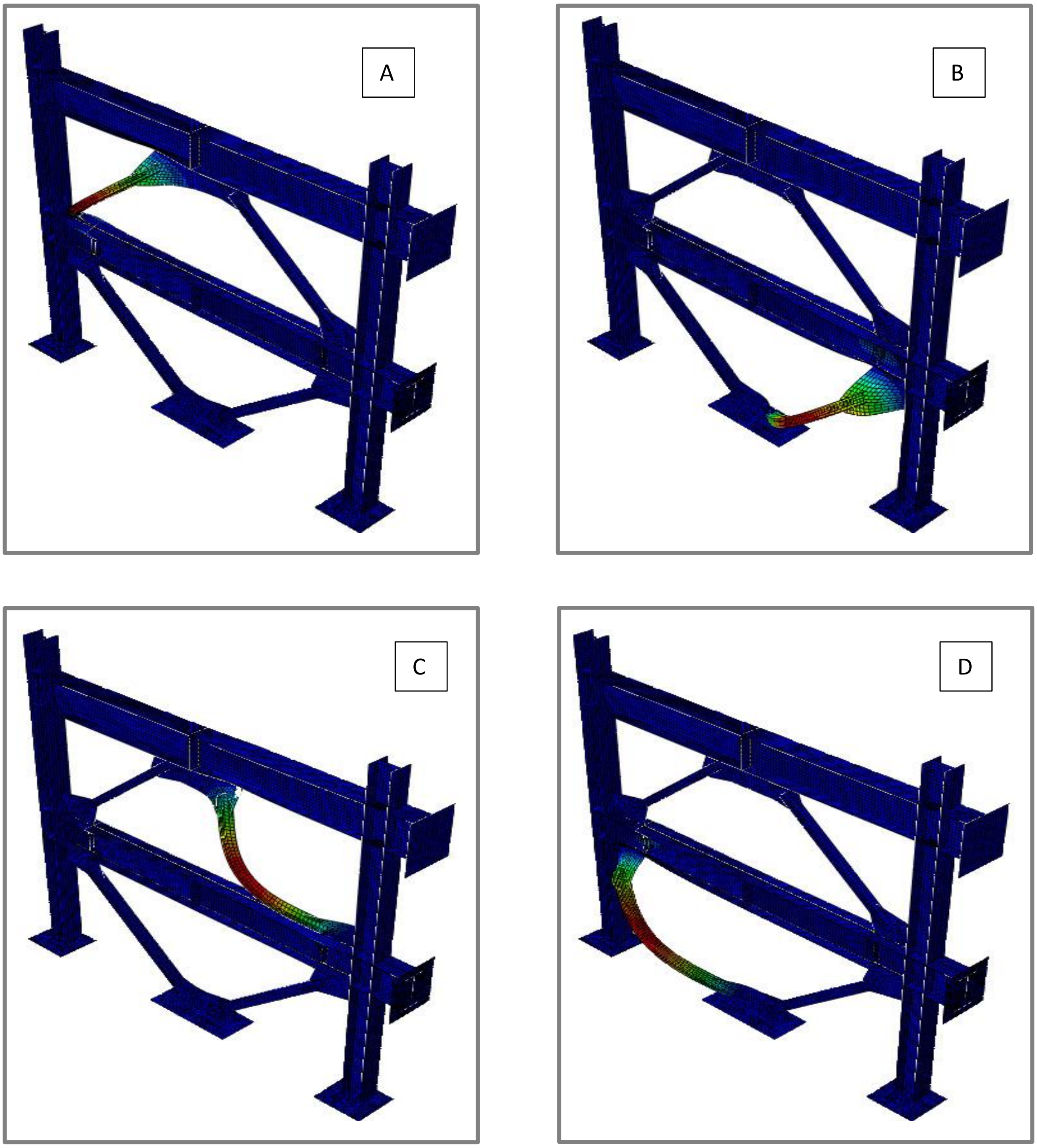

Fig. 17 : Buckling modes from buckling analysis by ABAQUS, where (A) is the first mode, (B) is the second mode, (C) is the third mode and (D) is the fourth mode.

3.7. VALIDATION OF FE MODEL

The FE Model was validated by comparing the analytical and experimental results. The FE model was loaded by two different types of loads, one of the loads was monotonic loading and the second was the cyclic loading

3.7.1. Comparison between roof displacement and base shear under the monotonic loading.

Fig. 18 shows the base shear vs. roof displacement for the experimental work and FE results. The FE model in this comparison was under the monotonic loading. As it can be seen from the figure, the FE model was yield at the same load of the experimental test which equal to 3100 kN which corresponds to a value of 25 mm of displacement approximately. After yielding at the same displacement of the value of 50 mm, the base shear of the FE model was less than the base shear of the experimental test by 2.5% approximately.

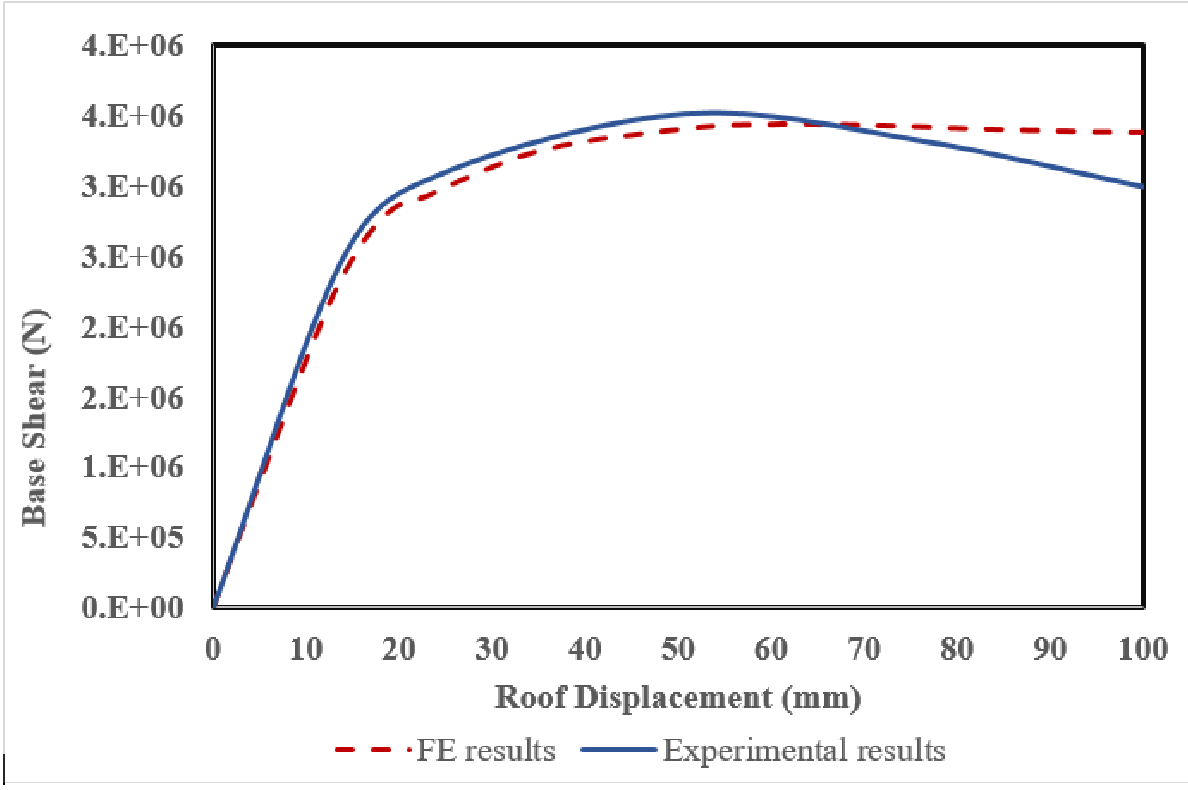

Fig. 18 : Comparing the FE results of ABAQUS versus experimental results under the monotonic loading.

3.7.2. Comparison between roof displacement and base shear under the cyclic loading.

Fig.19 shows the base shear vs. roof displacement for the experimental work and FE results under the cyclic loading. As it can be seen from the figure, the results of the FE model and experimental work in a good agreement

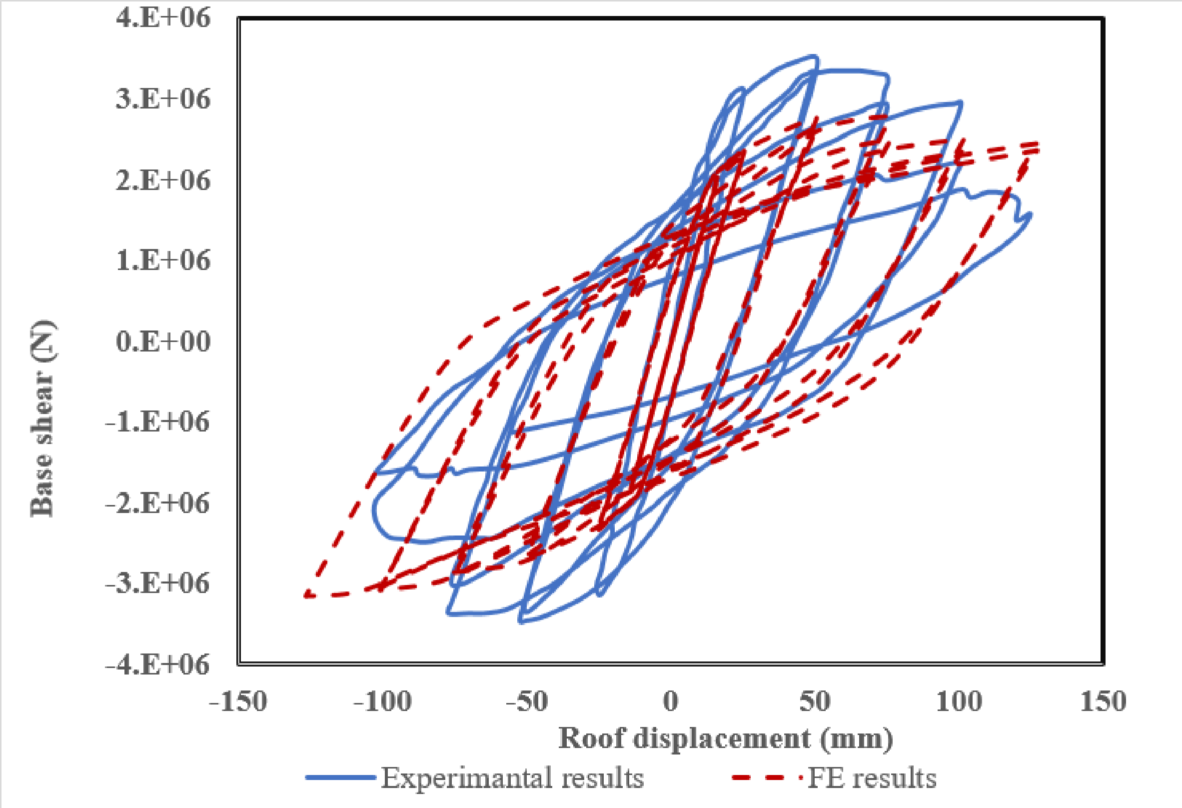

Fig.19 : Comparing the FE results of ABAQUS versus experimental results for the cyclic loading.

3.7.3. Comparison between the cyclic loading and the monotonic loading.

Fig. 20 shows the comparison between the cyclic and monotonic loading for the FE model and experimental work. As it can be seen from the figure, the monotonic and cyclic loading in a good agreement for the elastic range. After the elastic zone, there was a difference for the base shear at the same values for the displacement which equal to 50 mm where the base shear in the monotonic loading was higher than the base shear in the cyclic loading by 21% approximately. This means that the braced frame in case of FE model, if it is affected by a cyclic loading, collapses faster than if it is affected by a monotonic loading.

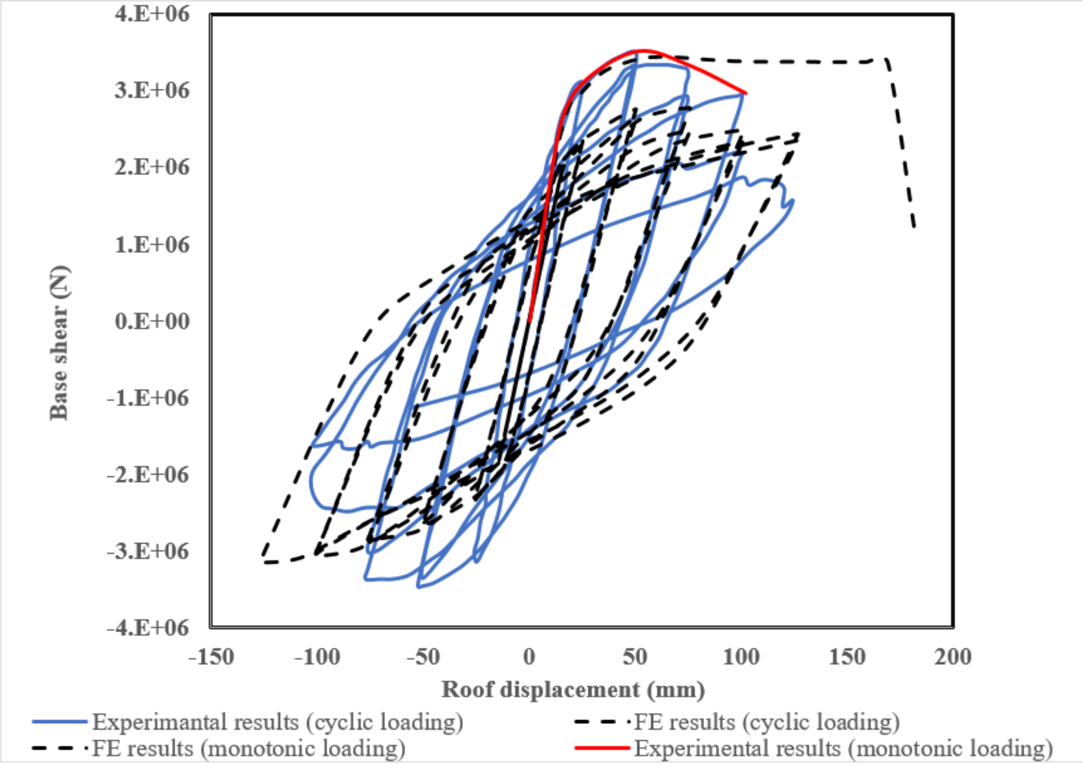

Fig. 20 : Comparing the cyclic loading versus monotonic loading for the FE results and experimental work.

SUMMARY

Steel braced frame systems are considered an efficient and economical lateral force resisting systems to control the lateral deformation in buildings under the wind and seismic loads. A three-dimensional finite element model for braced frame was developed to simulate the observed experimental test conducted by using ABAQUS/CAE (version 6.14-4). In the FE model, the loads were applied by two methods. The first method was the monotonic loading and the second method was the cyclic loading method. The FE Model was validated by comparing the analytical and experimental results. As it can be seen from the results, the FE model and experimental work in a good agreement.

REFERENCES

[1] Muir, L. S., & Thornton, W. A. AISC Steel Design Guide 29: Vertical Bracing Connections.

[2] ANSI/AISC 341-16. (2016). Seismic provisions for structural steel buildings. Seismic Provisions for Structural Steel Buildings, 60601.

[3] American Institute of Steel Construction. (1984). Engineering for Steel Construction. American Institute of Steel Construction.

[4] Richard, R. M. (1986, June). Analysis of large bracing connection designs for heavy construction. In National Steel Construction Conference Proceedings, American Institute of Steel Construction, Chicago, Illinois (pp. 31-7).

[5] Williams, g. C. (1986). Steel connection designs based on inelastic finite element analyses (gusset, bracing, structures). The university of Arizona.

[6] Astaneh, A. (1989). Simple methods for design of steel gusset plates. In Building Code Requirements for Masonry Structures (ACI 530-88/ASCE 5-88) and Specifications for Masonry Structures (ACI 530.1-88/ASCE 6-88)(ACI 530.1-88/ASCE 6-88) (pp. 345-354). ASCE.

[7] Thornton, W. A. (1991, June). On the analysis and design of bracing connections. In Proceedings AISC National Steel Construction Conference (pp. 26-1).

[8] Ricker, D. T. (1992). Value engineering and steel economy. Structural Steel Educational Council.

[9] Thornton, W. A. (1992). Designing for cost efficient fabrication. Structural Steel Educational Council.

[10] Astaneh-Asl, A. (1998). Seismic behavior and design of gusset plates. Structural Steel Educational Council.

[11] Muir, L. S. (2008). Designing compact gussets with the uniform force method. Engineering journal, 45(1), 13.

[12] Johnson, S. M. (2005). Improved seismic performance of special concentrically braced frames (Doctoral dissertation, University of Washington).

[13] Herman, D. (2006). Further improvements on and understanding of SCBF systems. MSCE thesis, University of Washington, Seattle.

[14] Kotulka, B. A. (2007). Analysis for a design guide on gusset plates used in special concentrically braced frames (Doctoral dissertation, University of Washington).

[15] Lumpkin, E. J. (2009). Enhanced seismic performance of multi-story special concentrically brace frames using a balanced design procedure (Doctoral dissertation, University of Washington).

[16] Powell, J. A. (2010). Evaluation of special concentrically braced frames for improved seismic performance and constructability (Doctoral dissertation, University of Washington).

[17] Roeder, C. W., Lumpkin, E. J., & Lehman, D. E. (2011). A balanced design procedure for special concentrically braced frame connections. Journal of Constructional Steel Research, 67(11), 1760-1772.

[18] Ebrahimi, S., Zahrai, S. M., & Mirghaderi, S. R. (2019). Numerical study on force transfer mechanism in through gusset plates of SCBFs with HSS columns & beams. Steel and Composite Structures, An International Journal, 31(6), 541-558.

[19] Lai, J. W. (2012). Experimental and analytical studies on the seismic behavior of conventional and hybrid braced frames (Doctoral dissertation, UC Berkeley).

[20] ABAQUS, H. (2014). ABAQUS standard user’s manual, version 6.14. Providence, RI, USA: Dassault System.